

Stearoyl-CoA desaturase regulates membrane biogenesis and hepatic merozoite formation in *Plasmodium berghei*

Satish Mishra¹, Sunil Narwal¹, Akancha Mishra¹, Ankit Ghosh¹, and Hadi Choudhary¹

¹CSIR-Central Drug Research Institute

August 16, 2023

Abstract

Plasmodium is an obligate intracellular parasite that requires intense lipid synthesis for membrane biogenesis and survival. One of the principal membrane components is oleic acid, which is required to maintain the membrane's biophysical properties and fluidity. The malaria parasite *Plasmodium* can modify fatty acids, and stearoyl-CoA $\Delta 9$ -desaturase (Scd) is an enzyme that catalyzes the synthesis of oleic acid by desaturation of stearic acid. Scd is dispensable in *P. falciparum* blood stages; however, its role in mosquito and liver stages remains unknown. We show that *P. berghei* Scd localizes to the ER in the blood and liver stages. Disruption of *Scd* in the rodent malaria parasite *P. berghei* did not affect parasite blood stage propagation, mosquito stage development, or early liver stage development. However, when *scd* KO sporozoites were inoculated intravenously or by mosquito bite into mice, they failed to initiate blood-stage infection. Immunofluorescence analysis revealed that organelle biogenesis was impaired and merozoite formation was abolished, which normally initiates blood-stage infections. Genetic complementation of the KO parasites restored merozoite formation to a level similar to that of WT parasites. Mice immunized with *Scd* KO sporozoites confer long-lasting sterile protection against infectious sporozoite challenge. Thus, the *Scd* KO parasite is an appealing candidate for inducing protective preerythrocytic immunity.

1. Introduction

Malaria infections caused by *Plasmodium* parasites continue to be the most important tropical disease that affects both animals and humans. Malaria was responsible for over 247 million cases and 619,000 deaths in 2021 (*World malaria report 2022*, 2022). *Plasmodium* sporozoite infection is initiated when an infected female *Anopheles* mosquito probes for the blood meal and deposits sporozoites in the skin. Sporozoites migrate to the liver to invade hepatocytes and initiate a replication cycle that generates thousands of hepatic merozoites to initiate an erythrocytic cycle (Prudêncio *et al.*, 2006; Lindner *et al.*, 2012). During these replicative stages, the parasite rapidly increases its biomass, which requires many nutrients, including lipids, for growth. Lipids are the most abundant components of any living organism and are essential for cell development and division. They are not only important for membrane biogenesis but are also major signaling molecules necessary for invasive stage formation (Mazumdar and Striepen, 2007). *Plasmodium* parasites can either obtain lipids from the host or synthesize them de novo to maintain propagation and survival within the host (Tarun *et al.*, 2009; Ramakrishnan *et al.*, 2013). However, de novo fatty acid synthesis is only essential in liver stages and is dispensable for the asexual blood stage because these stages can survive by scavenging fatty acids from the serum (Yu *et al.*, 2008; Vaughan *et al.*, 2009).

In apicomplexan parasites, the type II fatty acid synthesis (FAS II) pathway is localized to the apicoplast and catalyzed by four key enzymes, FabB/F, FabG, FabZ, and FabI (Marrakchi *et al.*, 2002; Ralph *et al.*, 2004; van Dooren and Striepen, 2013). *Plasmodium* parasites are also capable of modifying de novo synthesized or scavenged fatty acids into long unsaturated fatty acids (Gratraud *et al.*, 2009; Ramakrishnan *et al.*, 2015). An endoplasmic reticulum (ER)-localized stearoyl-CoA desaturase (Scd) was identified in *P. falciparum* that catalyzes the formation of oleic acid from stearic acid by the insertion of a cis double bond at the $\Delta 9$ position

of fatty acyl-CoAs (Shanklin *et al.* , 1994; Gratraud *et al.* , 2009). By using a *Scd* inhibitor, Gratraud *et al.* showed that methyl stercolate inhibits the synthesis of oleic acid and the development of asexual blood stage parasites (Gratraud *et al.* , 2009). Recently, *Scd* was found to be dispensable in a *P. falciparum* genetic screen (Zhang *et al.* , 2018); however, its role in mosquito and liver stages remains unknown.

The World Health Organization (WHO) recommended that the RTS,S vaccine (Zavala, 2022) might not be suitable for long-term usage because subunit vaccines occasionally do not elicit a strong or long-lasting immune response compared to whole-organism vaccines. Immunization with radiation-attenuated sporozoites (RAS) induces greater than 90% sterile protection in humans and has been the gold standard (Nussenzweig *et al.* , 1967). Repeated intravenous administration of RAS vaccines can achieve sterile protection in humans (Seder *et al.* , 2013). Immunization with live sporozoites attenuated by genetic modifications has gathered much attention, as they have been shown to produce protective immune responses equal to, or even greater than, those produced by irradiated sporozoites in rodent models (Khan *et al.* , 2012; Nganou-Makamdop and Sauerwein, 2013). GAPS offer several advantages over radiation-based attenuation, as they constitute a homogeneous population with a distinct genetic identity, and their attenuation is not dependent on external factors. Advances in *Plasmodium* genetics have enabled the generation of GAPS, which have overcome the limitations of RAS being used as a whole-organism vaccine. The obvious advantages of GAPS over RAS are that they are strategically generated by targeting genes, which are important for liver stage development, and that these KO lines are clonal lines inducing a uniform immune response owing to their block at one particular stage, i.e., early to mid-liver stage (Mueller *et al.* , 2005b; Mueller *et al.* , 2005a) or late liver stage (Ishino *et al.* , 2009; Dankwa *et al.* , 2016). These studies were extended to human parasites, where the success of *P. falciparum* GAP was shown (Murphy *et al.* , 2022). The protection of these attenuated sporozoite vaccines involves antibodies elicited against sporozoite antigens that neutralize their ability to invade hepatocytes (Seder *et al.* , 2013). Moreover, the protection is mediated through CD8+ T-cell responses that target infected hepatocytes (Epstein *et al.* , 2011).

Immunization of mice with late-arresting parasites (Butler *et al.* , 2011) resulted in a superior immune response and protection compared with early-arresting GAP (Aly *et al.* , 2008). It was shown that immunization with *P. falciparum* sporozoites under drug coverage allows parasites to mature into the late liver stage and elicit durable protection at lower doses compared to the *P. falciparum* RAS sporozoites vaccine (Mordmüller *et al.* , 2017). These data suggest that late-arresting GAP will be a superior immunogen and an ideal whole parasite vaccine. Although the arrested parasites are a source of antigen for effective priming of the immune system, their antigenic repertoire induces cross-stage immunity only when parasites experience a block at the late liver stage. Since late liver stages exhibit a subset of antigens that are common to blood stages, identifying genes that can yield a late-arresting mutant will have a broader impact on developing an efficacious GAP vaccine. Here, by using a genetically tractable model of *P. berghei* , we show that *Scd* is expressed during the blood and liver stages and is localized to the ER. To evaluate *Scd* function in mosquito and liver stages, we disrupted the gene, which resulted in impaired late liver-stage development that failed to initiate blood-stage infection. Immunization with *Scd*KO sporozoites protects against infectious sporozoite challenges.

2. Results

2.1 *P. berghei Scd* localized primarily in the endoplasmic reticulum

To study the expression and localization of *Scd* in the *P. berghei* life cycle, the gene was endogenously tagged with 3XHA by using double crossover homologous recombination (Fig. S1A). The correct integration of the targeting cassette at the *Scd* locus was confirmed by diagnostic PCR (Fig. S1B). Furthermore, the expression of *Scd*-3XHA was confirmed by western blotting using an anti-HA antibody (Fig. S1C). Transgenic parasites were analyzed throughout the parasite life cycle stages, and we found that the C-terminal tag did not affect parasite development (Fig. S1D and E). Previous studies have demonstrated the association of SCD with the endoplasmic reticulum (Gratraud *et al.* , 2009). By using *Pf Scd*-GFP transgenic parasites, it was shown that *P. falciparum* SCD localized to the ER in asexual blood stages. Similarly, we performed colocalization studies with the ER marker Bip and found that *P. berghei* was expressed in blood and liver stages and

primarily colocalized to the ER (Fig. 1A and B).

2. 2 *Scd* is not required for *P. berghei* blood and mosquito stage development

To address the function of *Scd*, we generated *Scd* KO parasites by using double crossover homologous recombination (Fig. S2A). After recombination, the *Scd* ORF was replaced by the GFP and hDHFR:yFCU expression cassettes, and GFP-expressing KO parasites were confirmed using fluorescence microscopy (Fig. S2B). The correct gene replacement was confirmed by diagnostic PCR, and clonal lines were obtained by limiting dilution of the parasites. The clonal lines were further confirmed by diagnostic PCR, and the absence of the *Scd* ORF was determined by locus PCR, which amplified 4.33 kb in WT GFP and 7.16 kb in *Scd* KO parasites (Fig. S2C). Furthermore, we confirmed the insertion of the targeting cassette at the correct locus by Southern blotting. The genomic DNA was digested with *EcoR* V and probed with a 5'UTR probe, which revealed a band of 3.28 kb in KO compared to 8.4 kb in WT GFP due to the presence of an *EcoR* V site in the GFP cassette (Fig. S2D). The *Scd*-complemented parasite line was also generated to check the specificity of the phenotype (Fig. S2E). For this, a *Scd* expression cassette consisting of the 5'UTR, ORF, and 3'UTR was amplified and transfected into *Scd* KO parasites. After recombination, the WT locus was amplified in *Scd* comp parasites (Fig. S2F). Next, we checked the effect of gene deletion on parasite growth during asexual blood stage propagation and found a similar growth pattern of WT GFP and KO parasites (Fig. S2G). To further understand the role of *Scd* in mosquito and liver stages, we transmitted the parasites to the mosquitoes by allowing mosquitoes to feed on infected mice. Examination on day 14 post feeding demonstrated normal development of oocysts and oocyst-derived sporozoites in the mosquito midgut (Fig. S3A-D). On days 18-22 post feeding, we observed intact salivary glands that showed a normal sporozoite load and a comparable number of salivary gland sporozoites in KO and WT GFP parasites (Fig. S3E and F). These results indicate that *Scd* is dispensable for parasite blood and mosquito stage development.

2. 3 *Scd* KO sporozoites infect the liver but fail to establish blood-stage infections in mice

To evaluate the role of *Scd* in liver stage development, different doses of WT and KO sporozoites were injected intravenously into C57BL/6 mice or infected by mosquito bite, and the appearance of the parasite in the blood was monitored by making a Giemsa blood smear. We found that all the mice injected with WT GFP and *Scd* comp became patent on day 3, whereas mice inoculated with KO sporozoites remained negative until the observation period (Table 1). The normal prepatent period of *Scd* comp parasites suggests that the lack of infectivity of KO parasites was due to the deletion of the *Scd* gene. To determine the stage-specific defect in KO parasites, we first investigated the invasion ability of KO sporozoites. For this, sporozoites were allowed to invade HepG2 cells, and sporozoites present inside and outside of the cells were counted, which revealed normal invasion by KO sporozoites (Fig. S4). Post invasion, sporozoites transform into EEFs that mature into merozoites, which are released 63 to 70 hpi in a controlled manner in the form of merozoites, and then the parasite biomass in the liver declines sharply (Sturm *et al.*, 2006). To analyze the progress of EEF development in vivo, the livers of infected mice were harvested at 36, 55, and 72 hpi, and parasite biomass was quantified by measuring 18S rRNA copy number using real-time PCR. We found that the 18S rRNA copy number was comparable in WT GFP and KO parasites at 36 hpi, but it was significantly lower at 55 hpi in KO parasites than in WT GFP parasites (Fig. 2A). However, the 18S rRNA copy number at 72 hpi was significantly lower in WT GFP than in KO (Fig. 2A), which suggested that mature WT GFP parasites egress from the liver but that KO parasites failed to mature and remained in the liver. We confirmed the maturation defect by determining the merozoite surface protein 1 (MSP1) transcripts at 55 hpi and found that it was significantly decreased in the KO parasites (Fig. 2B). These data provide evidence that *Scd* KO parasites failed to mature into hepatic merozoites and did not egress from hepatocytes.

2. 4 *Scd* KO liver stages grow normally but do not form hepatic merozoites

To further explore the *Scd* KO phenotype, HepG2 cells were infected with sporozoites, and the culture was fixed at different time points and stained with anti-UIS4 antibody and Hoechst. The *Scd*KO parasites grew similarly to the WT GFP parasites during liver stage development (Fig. 3A). We counted the EEF numbers and measured the size at 36, 48, and 62 hpi and found comparable numbers and sizes in *Scd* KO and WT

GFP parasites (Fig. 3B-G). Next, we checked the formation of merozoites by staining with an anti-MSP1 antibody. WT GFP showed nuclear segregation and merozoite formation, whereas there was abnormal DNA segregation in *Scd* KO parasites, and merozoite formation was abolished (Fig. 4A). We counted the nuclei in the EEF, which were found to be significantly fewer in *Scd* KO parasites (Fig. 4B). Next, we observed the culture for the formation of merosomes at 65 hpi and found it only in WT GFP (Fig. 4C). We counted the merosomes in WT GFP, and an equivalent amount of culture supernatant was injected into Swiss mice. The prepatent period was determined by making a Giemsa-stained blood smear. Mice injected with WT GFP merosomes became patent, whereas *Scd* KO supernatant-injected mice remained negative until the observation period (Table 2). This result suggests that *Scd* plays an important role in the maturation of hepatic merozoites and is essential for the liver-to-blood stage transition.

2. 5 Lack of *Scd* causes severe defects in organelle biogenesis

Lack of FAS II function in *Toxoplasma gondii* leads to defects in apicoplast biogenesis (Mazumdar *et al.* , 2006). To evaluate organelle morphology in *Scd* KO parasites, EEFs fixed at 62 hpi were immunostained with anti-ACP or anti-Bip antibodies to visualize the branching of the apicoplast and endoplasmic reticulum, respectively. We found normal branching of the apicoplast and endoplasmic reticulum in WT GFP parasites, whereas it was impaired in *Scd* KO parasites (Fig. 5A and B). Together, these results indicate that the FAS II pathway is essential for membrane biogenesis and parasite survival.

2. 6 Immunization with *Scd* KO sporozoites protects against malaria

Immunizations with sporozoites that arrest in the liver elicit a long-term protective host response and protect against infectious sporozoite challenge (Duffy, 2022). To study preerythrocytic protection induced by *Scd* KO parasites, groups of C57BL/6 mice were intravenously injected with three doses of sporozoites at intervals of two weeks and challenged with infectious sporozoites 10 days post-last immunization. All immunized mice remained blood stage negative after immunization, again demonstrating the lack of breakthrough blood stage infection. We found that all the mice injected with uninfected salivary gland debris developed blood-stage parasitemia, whereas mice immunized with *Scd* KO sporozoites were completely protected (Table 3). We further challenged the protected mice 120 days after the last immunization, and they remained protected (Table 3). These results demonstrate that immunization with *Scd* KO sporozoites induces preerythrocytic immunity and protects against malaria.

3 Discussion

The malaria parasite is an obligate intracellular parasite that scavenges the nutrients required to support its growth and replication from its host but also harbors enzymatic pathways for de novo synthesis of macromolecules. During its life cycle at different developmental stages, the parasite relies on its own biosynthetic machinery for cellular growth and proliferation. Lipid metabolism has emerged as a key regulator of cellular function and involves the synthesis of saturated fatty acids, which are further modified by desaturation and elongation (Shears *et al.* , 2015). *Scd* is an ER-localized enzyme involved in the desaturation of stearic acid into oleic acid to form unsaturated fatty acids (Gratraud *et al.* , 2009). In this study, we demonstrate that *P. berghei* *Scd* is not required for blood or mosquito stage development but is essential for liver stage development. The phenotype of *Scd* KO is similar to that of apicoplast-localized FASII pathway mutants, which were found to be essential for liver-stage development but not for blood-stage replication (Yu *et al.* , 2008; Vaughan *et al.* , 2009). The dispensability of the FASII pathway (Vaughan *et al.* , 2009) and desaturase enzyme *Scd* suggest that the *Plasmodium* parasite can scavenge lipids and saturated and unsaturated fatty acids directly from serum (Grellier *et al.* , 1991; Ofulla *et al.* , 1993). *Plasmodium* parasites directly utilize some FASII-generated fatty acids as lipid precursors without modification (Lindner *et al.* , 2014). However, the identification of apicoplast fatty acid export and the presence of desaturases and elongases in other cellular compartments suggested modification of fatty acids prior to incorporation into lipids (Ralph *et al.* , 2004; Mazumdar and Striepen, 2007; Gratraud *et al.* , 2009). This indicates that FASII-synthesized fatty acids are converted into a wide range of lipids for essential cellular function and that desaturation of fatty acids is an essential process for parasite development.

The FASII pathway enzymes and *Scd* were reported to be potential drug targets against the *P. falciparum* blood stage (Waller *et al.* , 2003; Gratraud *et al.* , 2009). However, previous reports and this study on lipid metabolism pathway mutants in *P. berghei* , *P. yoelii* , and *P. falciparum* suggest that FASII and *Scd* are not required for blood-stage development (Yu *et al.* , 2008; Vaughan *et al.* , 2009). Recently, *Scd* was found to be dispensable for the *P. falciparum* blood stage in a genetic screen (Zhang *et al.* , 2018). Further investigations are needed to determine why in vitro-maintained *P. falciparum* cultures are sensitive to FasII and *Scd* inhibitors. The normal development of *Scd* KO parasites in mosquitoes suggests that parasites can fulfill lipid requirements from this host as well. It is currently not known how the parasite utilizes mosquito lipids, but evidence suggests that host serum fatty acids are utilized by the parasite directly during blood stage development (Krishnegowda and Gowda, 2003; Mi-Ichi *et al.* , 2006). Deletion of the FASII enzymes *fabI* and *fabB/F* in *P. falciparum* abolished sporozoite development in mosquitoes, suggesting the essentiality of the FASII pathway during mosquito stage development (van Schaijk *et al.* , 2014). This may be an important distinction between human and rodent malaria parasites, where the FASII pathway is only implicated in liver stages (Vaughan *et al.* , 2009). The requirement of FASII during mosquito stage development in *P. falciparum* can be explained by the number of sporozoites produced per oocyst. Human malaria parasites *P. falciparum* and *P. vivax* produce approximately 3,400 and 3,700 sporozoites per oocyst compared to approximately 800 and 1,000 in *P. berghei* and *P. yoelii* , respectively (Rosenberg *et al.* , 1990; Shimizu *et al.* , 2010; Lindner *et al.* , 2013). Possibly, fatty acids required for the higher numbers of sporozoite production in human malaria parasites cannot be fulfilled by mosquitoes, and the parasite relies on its own biosynthetic machinery.

Similar to FAS II, *Scd* is essential for late liver-stage development and hepatic merozoite formation. It was documented that PVM protein UIS3 disruption leads to early attenuation of the parasite in the liver. UIS3 interacts with the hepatocyte lipid carrier liver-fatty acid binding protein (Mikolajczak *et al.* , 2007), and parasites may take up lipids through UIS3 from the host during early liver stage development. However, when the lipid requirement is high for membrane biogenesis during late liver stage development, import through UIS3 fails to fulfill the requirement (Baer *et al.* , 2007; Vaughan *et al.* , 2009), and the parasite switches to its own biosynthetic machinery. Alternatively, the *Scd*-derived oleic acid supply cannot be met by the host required for GPI biosynthesis for MSP1, which is a GPI-anchored protein (Gerold *et al.* , 1996). However, whether GPI biosynthesis is impaired in *Scd* KO parasites needs further investigation. The defects in organelles such as apicoplast and ER morphology and biogenesis in *Scd* KO parasites were possibly due to a lack of long-chain fatty acids. It was shown that both the apicoplast and the ER cooperate in the synthesis of very long fatty acids in *T. gondii* (Ramakrishnan *et al.* , 2012).

Immunizations with GAP sporozoites elicit a long-term protective host response (Overstreet *et al.* , 2008). We found that immunization with *Scd* KO sporozoites in mice conferred complete protection against WT sporozoite challenge. Interestingly, GAPs that arrest late in the liver stage provide superior protection compared to early-arresting GAPs (Butler *et al.* , 2011). Because immunization using late-liver-stage arresting GAP expresses late-stage antigens and blood-stage overlapping antigens, whether *Scd* GAP induces superior protection needs further investigation. Despite the discovery of a growing list of GAPs, there have been some occasional breakthrough infections in a few GAPs. Breakthrough infections have been reported with previously reported GAP sporozoites (Kumar *et al.* , 2016). Multiple gene deletion GAPs can be created to overcome these limitations by combining them with known GAPs (Yu *et al.* , 2008; Vaughan *et al.* , 2009; Dankwa *et al.* , 2016). Multiple gene deletions prevent breakthrough infections that engender these parasites with a higher degree of attenuation to prevent any possible breakthrough infection (Mikolajczak *et al.* , 2014).

In conclusion, we have provided evidence that *Scd* is essential for the liver-to-blood stage transition. *Scd* disruption results in impaired organelle biogenesis and complete loss of hepatic merozoite formation. Immunization with *Scd* KO sporozoites protects against WT sporozoite challenge and could be used as a potential GAP vaccine.

4 Materials and Methods

4. 1 Parasites and mice

P. berghei ANKA (MRA 311) and *P. berghei* ANKA GFP (MRA 867 507 m6c11) were obtained from BEI resources, USA. Swiss albino and C57BL/6 mice were used for parasite infections. All animal experiments performed in this study were approved by the Institutional Animal Ethics Committee at CSIR-Central Drug Research Institute, India (IAEC reference no: IAEC/2013/83).

4. 2 Generation of Scd-3XHA transgenic parasites

For the 3XHA tagging of the stearyl-CoA desaturase (*Scd*) (*Pb* ANKA_1110700) gene, two fragments, F1 (0.773 kb) and F2 (0.584 kb), were amplified from *P. berghei* genomic DNA using primers 1045/1055 and 1041/1042 and cloned into the pBC-3XHA-hDHFR vector at *Xho* I/*Bgl* II and *Not* I/*Asc* I, respectively. The construct was linearized with *Xho* I/*Asc* I and transfected into *P. berghei* ANKA schizonts as previously described (Janse *et al.*, 2006). The resistant parasites were selected using pyrimethamine (Sigma, USA), and genomic DNA was isolated using a genomic DNA isolation kit (Promega, USA). Correct 5' and 3' site-specific integration was confirmed by diagnostic PCR using primer pairs 1043/1218 and 1215/1044, respectively (primer sequences are given in Table S1). For the localization of *Scd* in the blood stage, transgenic *Scd*-3XHA-infected blood was spotted on 12-well slides (Thermo Fisher Scientific, USA) and fixed with 4% paraformaldehyde.

4. 3 Western blot analysis

For the analysis of the *Scd*-3XHA fusion protein in transgenic parasites, blood-stage parasites were harvested, washed three times with PBS, and pelleted by centrifugation. The iRBC pellet was lysed using 0.15% saponin, and the released parasites were pelleted, washed with PBS containing complete protease inhibitors (Roche, Switzerland), and resuspended in Laemmli buffer. Immunoblotting was performed as previously described (Narwal *et al.*, 2022). Briefly, samples were resolved on SDS-PAGE and transferred onto nitrocellulose membranes (Bio-Rad, USA), blocked with 5% nonfat dry milk in PBS, and incubated with anti-HA antibody (diluted 1:1,000, Novus Biologicals, USA) followed by incubation with HRP-conjugated anti-rabbit IgG (diluted 1:5,000, Amersham Biosciences, United Kingdom). The signals were detected using ECL chemiluminescent substrate (Thermo Scientific, USA) in a ChemiDoc XRS+ System (Bio-Rad, USA).

4. 4 Mosquito cycles

Anopheles stephensi mosquitoes were maintained as previously described (Narwal *et al.*, 2022). To obtain sporozoites, mosquitoes were allowed to feed on infected Swiss mice, and cages were kept in an environmental chamber maintained at 190degC with 80% relative humidity. The development of oocysts was observed on day 14, and salivary gland sporozoites were dissected between days 18-22 postfeeding.

4. 5 Generation of *Scd* knockout (*Scd* KO) and complemented (*Scd* comp) parasites

The *Scd* (*Pb* ANKA_1110700) targeting vector was constructed by cloning two PCR products, F3 (578 bp) and F4 (573 bp), into the pBC-GFP-hDHFR:yFCU plasmid at *Xho* I/*Sal* I and *Not* I/*Asc* I, respectively. The fragments F3 and F4 were amplified from *P. berghei* ANKA genomic DNA using primer pairs 1039/1056 and 1041/1042, respectively. The final vector was digested with *Xho* I/*Asc* I and transfected into *P. berghei* schizonts as previously described (Janse *et al.*, 2006). Genomic DNA was isolated from the drug-resistant GFP-expressing parasites, and correct 5' and 3' site-specific integration was confirmed by diagnostic PCR using primers 1410/1225 and 1215/1044, respectively. Clonal lines were obtained by limiting dilution of the parasite and again confirmed for integration by PCR. The modified genomic locus was confirmed by PCR using primers 1410/1044. For Southern blotting, parasite genomic DNA was digested with *EcoR* V, run on a 0.7% agarose gel, transferred to a positively charged nylon membrane (Amersham Biosciences, United Kingdom) and developed as previously described (Narwal *et al.*, 2022). The membrane was probed with a digoxigenin-labeled 5' probe (DIG High Prime DNA labeling and detection kit, Roche Applied Sciences, Switzerland). To generate a *Scd* KO complemented parasite line, a fragment consisting of the *Scd* 5'UTR, ORF, and 3'UTR was amplified using primers 1410/1044 and transfected into *Scd* KO parasites. Parasites containing restored *Scd* loci were selected by negative selection using a 5-fluorocytosine (5-FC) drug (Sigma, USA) as previously described (Srivastava and Mishra, 2022). Negative selection selects

parasites lacking the hDHFR:γFCU cassette. The complemented line was confirmed by the absence of GFP fluorescence and amplification of the *Scd* expression cassette by diagnostic PCR using primers 1410/1044.

4. 6 Determination of the *Scd* KO phenotype

Phenotypic analyses of the *Scd* KO parasites were performed as previously described (Srivastava and Mishra, 2022). Asexual blood growth was monitored by intravenously injecting 200 μl of blood with 0.2% parasitemia into two groups of Swiss albino mice (n=4). Parasitemia was determined by counting Giemsa-stained blood smears. The WT and *Scd* KO sporozoites were isolated from the infected mosquito's salivary glands on days 18-22 post blood meal and counted using a hemocytometer. For the determination of in vivo infectivity, C57BL/6 mice were either intravenously inoculated with salivary gland sporozoites or infected by mosquito bite, and blood-stage infection was monitored by making Giemsa-stained blood smears. Another group of mice injected with 5,000 sporozoites was sacrificed at 36, 55, and 72 hpi, and the livers were harvested and homogenized in TRIzol reagent (Invitrogen, USA). For the invasion assay, HepG2 cells were infected with salivary gland sporozoites (10,000/well) and culture fixed after 1 h and stained with anti-CSP antibody (Yoshida *et al.*, 1980) before and after permeabilization as described (Rénia *et al.*, 1988). The detailed EEF development assay was performed as previously described (Srivastava and Mishra, 2022). Briefly, HepG2 cells (5.5×10^4) were seeded in a 48-well plate containing collagen-coated coverslips and incubated overnight at 37°C in a CO₂ incubator. Salivary gland sporozoites (5,000/well) were added and incubated at 37°C, and the culture was fixed using 4% paraformaldehyde (PFA) at different time points. For the merosome assay, HepG2 cells (100,000/well) were seeded in a 24-well plate, infected with salivary gland sporozoites (40,000/well), and harvested at 65 hpi to count the merosome numbers. Merosomes were injected into Swiss mice to check the infectivity.

4. 7 Real-time PCR assays for quantification of parasites

Total RNA was isolated from the infected liver, and cDNA was synthesized as previously described (Choudhary *et al.*, 2019). The parasite burden was quantified by amplifying 18S rRNA (Bruña-Romero *et al.*, 2001) using primers 1195/1196. MSP1 transcripts were quantified using primers 1219/1220. Liver samples were normalized to mouse glyceraldehyde-3-phosphate dehydrogenase (GAPDH) using primers 1193/1194. To quantify the copy number, gene-specific standards were run alongside the unknown samples.

4. 8 Immunofluorescence Assay

IFA was performed as described previously (Narwal *et al.*, 2022). The PFA-fixed cells were washed twice with PBS, and blood-stage parasites were permeabilized with 0.1% Triton-X100 in PBS for 10 min and liver stages in chilled methanol for 20 min at 4°C and blocked with 1% BSA-PBS. The cells were incubated for 1 h with the following primary antibodies: anti-HA antibody (diluted 1:1,000, Novus Biologicals, USA), anti-BiP (diluted 1:125, MRA-1246, BEI resources), anti-UIS4 (diluted 1:1,000 (Mueller *et al.*, 2005b), anti-merozoite surface protein 1 (MSP1) monoclonal antibody (diluted 1:5000 (Holder and Freeman, 1981), and anti-acyl carrier protein (ACP, diluted 1:800) (Gallagher and Prigge, 2010). The signals were visualized with secondary antibodies: Alexa Fluor 594-conjugated anti-rabbit IgG (diluted 1:500; Invitrogen, USA), Alexa Fluor 488-conjugated anti-mouse IgG (diluted 1:500; Invitrogen, USA), and Alexa Fluor 488-conjugated anti-rabbit IgG (diluted 1:500; Invitrogen, USA). The nuclei were stained with Hoechst, and the coverslips were mounted using Prolong Diamond antifade reagent (Thermo Scientific, USA). Images were acquired using FV1000 software on a confocal laser scanning microscope (Olympus BX61WI) equipped with a UPlanSAPO 100x/1.4 oil immersion objective. The EEFs were counted manually, and the area was measured using Nikon NIS elements BR imaging software under an Eclipse 80i fluorescence microscope/Plan Fluor 40x/0.75 objective.

4. 9 Immunization and challenge experiment

Female C57BL/6 mice (6-8 weeks old) were intravenously injected with three doses of salivary gland sporozoites at an interval of two weeks. Control groups were injected with uninfected mosquito salivary gland debris. Both groups were challenged with 5,000 WT sporozoites 10 post last immunization. The appearance

of parasites in blood was monitored by making Giemsa-stained blood smears.

4. 10 Statistical analysis

Statistical analysis was carried out in GraphPad Prism software using two-tailed, unpaired Student's t test or one-way ANOVA.

Acknowledgments

We thank BEI resources, USA, for the parasite strains and plasmids. We thank Dr. Kota Arun Kumar (University of Hyderabad, India) for the pBC-3XHA-hDHFR vector. We thank Dr. Anthony A. Holder (The Francis Crick Institute, UK), Drs. Photini Sinnis and Sean Prigge (Johns Hopkins University, USA) for anti-MSP1, anti-UIS4, and anti-ACP antibodies, respectively. We acknowledge the THUNDER (BSC0102) and MOES (GAP0118) Intravital and Confocal microscopy facility of CSIR-CDRI. The Indian Council of Medical Research, University Grants Commission, and Council of Scientific and Industrial Research, Government of India research fellowships supported SKN, AM, HHC, and AG.

Conflict of interest

The authors declare that they have no conflicts of interest.

Author contributions

SKN and SM conceived the idea, designed and performed the experiments, analyzed the data and wrote the manuscript. AM, AG, and HHC performed the experiments. All the authors have read and approved the manuscript.

Declarations

Ethics approval

The current study does not involve human samples. All animal procedures conducted were approved by the Institutional Animal Ethics Committee at CSIR-Central Drug Research Institute, India (IAEC/2013/83).

Consent to participate

Not applicable.

Consent for publication

Not applicable.

Availability of data and material

All data are available within this manuscript, and raw data are available from the corresponding author upon reasonable request. Materials generated in this study are available from the corresponding author upon request.

Funding

The work was supported by the Ramalingaswami Fellowship grant (BT/RLF/Re-entry/20/2012).

Authors' information

Division of Molecular Microbiology and Immunology, CSIR-Central Drug Research Institute, Lucknow 226031, India.

Sunil Kumar Narwal, Akancha Mishra, Ankit Ghosh, Hadi Hasan Choudhary, Satish Mishra

Academy of Scientific and Innovative Research (AcSIR), Ghaziabad 201002, India.

Akancha Mishra, Satish Mishra

References

- Aly, A.S.I., Mikolajczak, S.A., Rivera, H.S., Camargo, N., Jacobs-Lorena, V., Labaied, M., *et al.* (2008) Targeted deletion of SAP1 abolishes the expression of infectivity factors necessary for successful malaria parasite liver infection. *Mol Microbiol* **69** : 152–163.
- Baer, K., Klotz, C., Kappe, S.H.I.I., Schnieder, T., and Frevert, U. (2007) Release of hepatic *Plasmodium yoelii* merozoites into the pulmonary microvasculature. *PLoS Pathog* **3** : 1651–1668.
- Bruna-Romero, O., Hafalla, J.C., Gonzalez-Aseguinolaza, G., Sano, G., Tsuji, M., and Zavala, F. (2001) Detection of malaria liver-stages in mice infected through the bite of a single *Anopheles* mosquito using a highly sensitive real-time PCR. *Int J Parasitol* **31** : 1499–1502.
- Butler, N.S., Schmidt, N.W., Vaughan, A.M., Aly, A.S., Kappe, S.H.I.I., and Harty, J.T. (2011) Superior antimalarial immunity after vaccination with late liver stage-arresting genetically attenuated parasites. *Cell Host Microbe* **9** : 451–462.
- Choudhary, H.H., Gupta, R., and Mishra, S. (2019) PKAc is not required for the preerythrocytic stages of *Plasmodium berghei*. **2** : 1–11.
- Dankwa, D.A., Davis, M.J., Kappe, S.H.I., and Vaughan, A.M. (2016) A *Plasmodium yoelii* Mei2-like RNA binding protein is essential for completion of liver stage schizogony. *Infect Immun* **84** : 1336–1345.
- Dooren, G.G. van, and Striepen, B. (2013) The algal past and parasite present of the apicoplast. *Annu Rev Microbiol* **67** : 271–289.
- Duffy, P.E. (2022) Current approaches to malaria vaccines. *Curr Opin Microbiol* **70** : 102227.
- Epstein, J.E., Tewari, K., Lyke, K.E., Sim, B.K.L., Billingsley, P.F., Laurens, M.B., *et al.* (2011) Live attenuated malaria vaccine designed to protect through hepatic CD8⁺ T cell immunity. *Science* **334** : 475–480.
- Gallagher, J.R., and Prigge, S.T. (2010) *Plasmodium falciparum* acyl carrier protein crystal structures in disulfide-linked and reduced states and their prevalence during blood stage growth. *Proteins* **78** : 575–588.
- Gerold, P., Schofield, L., Blackman, M.J., Holder, A.A., and Schwarz, R.T. (1996) Structural analysis of the glycosyl-phosphatidylinositol membrane anchor of the merozoite surface proteins-1 and -2 of *Plasmodium falciparum*. *Mol Biochem Parasitol* **75** : 131–143.
- Gratraud, P., Huws, E., Falkard, B., Adjalley, S., Fidock, D.A., Berry, L., *et al.* (2009) Oleic acid biosynthesis in *Plasmodium falciparum*: characterization of the stearyl-CoA desaturase and investigation as a potential therapeutic target. *PLoS One* **4** : e6889.
- Grellier, P., Rigomier, D., Clavey, V., Fruchart, J.C., and Schrevel, J. (1991) Lipid traffic between high density lipoproteins and *Plasmodium falciparum*-infected red blood cells. *J Cell Biol* **112** : 267–277.
- Holder, A.A., and Freeman, R.R. (1981) Immunization against blood-stage rodent malaria using purified parasite antigens. *Nature* **294** : 361–364.
- Ishino, T., Boisson, B., Orito, B.B., Lacroix, C., Bischoff, E., Loussert, C., *et al.* (2009) LISP1 is important for the egress of *Plasmodium berghei* parasites from liver cells. *Cell Microbiol* **11** : 1329–1339.
- Janse, C.J., Ramesar, J., and Waters, A.P. (2006) High-efficiency transfection and drug selection of genetically transformed blood stages of the rodent malaria parasite *Plasmodium berghei*. *Nat Protoc* **1** : 346–356.
- Khan, S.M., Janse, C.J., Kappe, S.H.I., and Mikolajczak, S.A. (2012) Genetic engineering of attenuated malaria parasites for vaccination. *Curr Opin Biotechnol* **23** : 908–916 <http://dx.doi.org/10.1016/j.copbio.2012.04.003>.
- Krishnegowda, G., and Gowda, D.C. (2003) Intraerythrocytic *Plasmodium falciparum* incorporates extraneous fatty acids to its lipids without any structural modification. *Mol Biochem Parasitol* **132** : 55–58.

- Kumar, H., Sattler, J.M., Singer, M., Heiss, K., Reinig, M., Hammerschmidt-Kamper, C., *et al.* (2016) Protective efficacy and safety of liver stage attenuated malaria parasites. *Sci Rep* **6** : 1–9 <http://dx.doi.org/10.1038/srep26824>.
- Lindner, S.E., Mikolajczak, S.A., Vaughan, A.M., Moon, W., Joyce, B.R., Sullivan, W.J., and Kappe, S.H.I. (2013) Perturbations of Plasmodium Puf2 expression and RNA-seq of Puf2-deficient sporozoites reveal a critical role in maintaining RNA homeostasis and parasite transmissibility. *Cell Microbiol* **15** : 1266–1283.
- Lindner, S.E., Miller, J.L., and Kappe, S.H.I. (2012) Malaria parasite pre-erythrocytic infection: Preparation meets opportunity. *Cell Microbiol* **14** : 316–324.
- Lindner, S.E., Sartain, M.J., Hayes, K., Harupa, A., Moritz, R.L., Kappe, S.H.I., and Vaughan, A.M. (2014) Enzymes involved in plastid-targeted phosphatidic acid synthesis are essential for Plasmodium yoelii liver-stage development. *Mol Microbiol* **91** : 679–693.
- Marrakchi, H., Zhang, Y.M., and Rock, C.O. (2002) Mechanistic diversity and regulation of Type II fatty acid synthesis. *Biochem Soc Trans* **30** : 1050–1055.
- Mazumdar, J., and Striepen, B. (2007) Make it or take it: fatty acid metabolism of apicomplexan parasites. *Eukaryot Cell* **6** : 1727–1735.
- Mazumdar, J., Wilson, E.H., Masek, K., Hunter, C.A., and Striepen, B. (2006) Apicoplast fatty acid synthesis is essential for organelle biogenesis and parasite survival in Toxoplasma gondii. *Proc Natl Acad Sci U S A* **103** : 13192–13197.
- Mi-Ichi, F., Kita, K., and Mitamura, T. (2006) Intraerythrocytic Plasmodium falciparum utilize a broad range of serum-derived fatty acids with limited modification for their growth. *Parasitology* **133** : 399–410.
- Mikolajczak, S.A., Jacobs-Lorena, V., MacKellar, D.C., Camargo, N., and Kappe, S.H.I. (2007) L-FABP is a critical host factor for successful malaria liver stage development. *Int J Parasitol* **37** : 483–489.
- Mikolajczak, S.A., Lakshmanan, V., Fishbaugher, M., Camargo, N., Harupa, A., Kaushansky, A., *et al.* (2014) A next-generation genetically attenuated Plasmodium falciparum parasite created by triple gene deletion. *Mol Ther* **22** : 1707–1715.
- Mordmuller, B., Surat, G., Lagler, H., Chakravarty, S., Ishizuka, A.S., Lalremruata, A., *et al.* (2017) Sterile protection against human malaria by chemoattenuated PfSPZ vaccine. *Nature* **542** : 445–449 <http://dx.doi.org/10.1038/nature21060>.
- Mueller, A.-K., Labaied, M., Kappe, S.H.I., and Matuschewski, K. (2005a) Genetically modified Plasmodium parasites as a protective experimental malaria vaccine. *Nature* **433** : 164–167.
- Mueller, A.K., Camargo, N., Kaiser, K., Andorfer, C., Frevert, U., Matuschewski, K., and Kappe, S.H.I. (2005b) Plasmodium liver stage developmental arrest by depletion of a protein at the parasite-host interface. *Proc Natl Acad Sci U S A* **102** : 3022–3027.
- Murphy, S.C., Vaughan, A.M., Kublin, J.G., Fishbauger, M., Seilie, A.M., Cruz, K.P., *et al.* (2022) A genetically engineered Plasmodium falciparum parasite vaccine provides protection from controlled human malaria infection. *Sci Transl Med* **14** : eabn9709.
- Narwal, S.K., Nayak, B., Mehra, P., and Mishra, S. (2022) Protein kinase 9 is not required for completion of the Plasmodium berghei life cycle. *Microbiol Res* **260** : 127051.
- Nganou-Makamdop, K., and Sauerwein, R.W. (2013) Liver or blood-stage arrest during malaria sporozoite immunization: the later the better? *Trends Parasitol* **29** : 304–310 <http://dx.doi.org/10.1016/j.pt.2013.03.008>.
- Nussenzweig, R.S., Vanderberg, J., Most, H., and Orton, C. (1967) Protective immunity produced by the injection of x-irradiated sporozoites of plasmodium berghei. *Nature* **216** : 160–162.

- Ofulla, A. V., Okoye, V.C., Khan, B., Githure, J.I., Roberts, C.R., Johnson, A.J., and Martin, S.K. (1993) Cultivation of *Plasmodium falciparum* parasites in a serum-free medium. *Am J Trop Med Hyg* **49** : 335–340.
- Overstreet, M.G., Cockburn, I.A., Chen, Y.C., and Zavala, F. (2008) Protective CD8+ T cells against *Plasmodium* liver stages: Immunobiology of an “unnatural” immune response. *Immunol Rev* **225** : 272–283.
- Prudencio, M., Rodriguez, A., and Mota, M.M. (2006) The silent path to thousands of merozoites: The *Plasmodium* liver stage. *Nat Rev Microbiol* **4** : 849–856.
- Ralph, S.A., Dooren, G.G. van, Waller, R.F., Crawford, M.J., Fraunholz, M.J., Foth, B.J., *et al.* (2004) Tropical infectious diseases: metabolic maps and functions of the *Plasmodium falciparum* apicoplast. *Nat Rev Microbiol* **2** : 203–216.
- Ramakrishnan, S., Docampo, M.D., MacRae, J.I., Pujol, F.M., Brooks, C.F., Dooren, G.G. Van, *et al.* (2012) Apicoplast and endoplasmic reticulum cooperate in fatty acid biosynthesis in apicomplexan parasite *Toxoplasma gondii*. *J Biol Chem* **287** : 4957–4971.
- Ramakrishnan, S., Docampo, M.D., MacRae, J.I., Ralton, J.E., Rupasinghe, T., McConville, M.J., and Striepen, B. (2015) The intracellular parasite *Toxoplasma gondii* depends on the synthesis of long-chain and very long-chain unsaturated fatty acids not supplied by the host cell. *Mol Microbiol* **97** : 64–76.
- Ramakrishnan, S., Serricchio, M., Striepen, B., and Butikofer, P. (2013) Lipid synthesis in protozoan parasites: a comparison between kinetoplastids and apicomplexans. *Prog Lipid Res* **52** : 488–512.
- Renia, L., Miltgen, F., Charoenvit, Y., Ponnudurai, T., Verhave, J.P., Collins, W.E., and Mazier, D. (1988) Malaria sporozoite penetration A new approach by double staining. *J Immunol Methods* **112** : 201–205.
- Rosenberg, R., Wirtz, R.A., Schneider, I., and Burge, R. (1990) An estimation of the number of malaria sporozoites ejected by a feeding mosquito. *Trans R Soc Trop Med Hyg* **84** : 209–212.
- Schajjk, B.C.L. van, Kumar, T.R.S., Vos, M.W., Richman, A., Gemert, G.-J. van, Li, T., *et al.* (2014) Type II fatty acid biosynthesis is essential for *Plasmodium falciparum* sporozoite development in the midgut of *Anopheles* mosquitoes. *Eukaryot Cell* **13** : 550–559.
- Seder, R.A., Chang, L.-J.J., Enama, M.E., Zephir, K.L., Sarwar, U.N., Gordon, I.J., *et al.* (2013) Protection against malaria by intravenous immunization with a nonreplicating sporozoite vaccine. *Science (80-)* **341** : 1359–1365.
- Shanklin, J., Whittle, E., and Fox, B.G. (1994) Eight histidine residues are catalytically essential in a membrane-associated iron enzyme, stearoyl-CoA desaturase, and are conserved in alkane hydroxylase and xylene monooxygenase. *Biochemistry* **33** : 12787–12794.
- Shears, M.J., Botte, C.Y., and McFadden, G.I. (2015) Fatty acid metabolism in the *Plasmodium* apicoplast: Drugs, doubts and knockouts. *Mol Biochem Parasitol* **199** : 34–50 <http://dx.doi.org/10.1016/j.molbiopara.2015.03.004>.
- Shimizu, S., Osada, Y., Kanazawa, T., Tanaka, Y., and Arai, M. (2010) Suppressive effect of azithromycin on *Plasmodium berghei* mosquito stage development and apicoplast replication. *Malar J* **9** : 73.
- Srivastava, P.N., and Mishra, S. (2022) Disrupting a *Plasmodium berghei* putative phospholipase impairs efficient egress of merozoites. *Int J Parasitol* **52** : 547–558 <https://doi.org/10.1016/j.ijpara.2022.03.002>.
- Sturm, A., Amino, R., Sand, C. Van De, Regen, T., Retzlaff, S., Rennenberg, A., *et al.* (2006) Manipulation of host hepatocytes by the malaria parasite for delivery into liver sinusoids. *Science (80-)* **313** : 1287–1290.
- Tarun, A.S., Vaughan, A.M., and Kappe, S.H.I. (2009) Redefining the role of de novo fatty acid synthesis in *Plasmodium* parasites. *Trends Parasitol* **25** : 545–550.

Vaughan, A.M., O'Neill, M.T., Tarun, A.S., Camargo, N., Phuong, T.M., Aly, A.S.I.I., *et al.* (2009) Type II fatty acid synthesis is essential only for malaria parasite late liver stage development. *Cell Microbiol* **11** : 506–520.

Waller, R.F., Ralph, S.A., Reed, M.B., Su, V., Douglas, J.D., Minnikin, D.E., *et al.* (2003) A type II pathway for fatty acid biosynthesis presents drug targets in *Plasmodium falciparum*. *Antimicrob Agents Chemother* **47** : 297–301.

World malaria report 2022 (2022) .

Yoshida, N., Nussenzweig, R.S., Potocnjak, P., Nussenzweig, V., and Aikawa, M. (1980) Hybridoma Produces Protective Antibodies Directed against the Sporozoite Stage of Malaria Parasite. *Science (80-)* **207** : 71–73.

Yu, M., Kumar, T.R.S., Nkrumah, L.J., Coppi, A., Retzlaff, S., Li, C.D., *et al.* (2008) The fatty acid biosynthesis enzyme FabI plays a key role in the development of liver-stage malarial parasites. *Cell Host Microbe* **4** : 567–578.

Zavala, F. (2022) RTS,S: the first malaria vaccine. *J Clin Invest* **132** .

Zhang, M., Wang, C., Otto, T.D., Oberstaller, J., Liao, X., Adapa, S.R., *et al.* (2018) Uncovering the essential genes of the human malaria parasite *Plasmodium falciparum* by saturation mutagenesis. *Science (80-)* **360** .

Table 1. Infectivity of salivary gland sporozoites in C57BL/6 mice. NA, Not applicable.

Experiment	Parasite	Number of sporozoites inoculated	Mice positive/mice inoculated	Prepatent per
1	WT	5,000	10/10	3
	<i>Scd</i> KO	5,000	0/15	NA
	<i>Scd</i> comp	5,000	5/5	3
2	WT	10,000	10/10	3
	<i>Scd</i> KO	10,000	0/20	NA
	<i>Scd</i> KO	20,000	0/10	NA
	<i>Scd</i> comp	10,000	5/5	3
	WT	From 20 mosquitos	5/5	3
	<i>Scd</i> KO	From 20 mosquitos	0/5	NA
3	WT	50,000	5/5	3
	<i>Scd</i> KO	50,000	0/10	NA

Table 2. Infectivity of merosomes in Swiss mice. NA, Not applicable.

Experiment	Parasite	Number of merosomes injected	Mice positive/mice injected	Prepatent period (d)
1	WT	1	5/5	6
	<i>Scd</i> KO	Spernatant	0/5	NA
2	WT	10	5/5	2
	<i>Scd</i> KO	Spernatant	0/5	NA

Table 3. Immunization of C57BL/6 mice by intravenous injection of *Scd* KO sporozoites. All immunized mice were protected from WT *P. berghei* sporozoite challenge. NA, Not applicable

Experiment	Group	Immunization dose	Challenge day	Challenge dose	No. of patent/no. of challenged	Prepatent period (day)
1	Control	(3x) SG debris	10	5,000	5/5	3
	<i>Scd</i> KO	(1x) 5x10 ⁴ and (2x) 2.5x10 ⁴	10	5,000	0/5	NA
2	Control	(3x) SG debris	10	5,000	5/5	3
	<i>Scd</i> KO	(1x) 5x10 ⁴ and (2x) 2.5x10 ⁴	10 120	5,000 5,000	0/5 0/5	NA NA

Figure legends

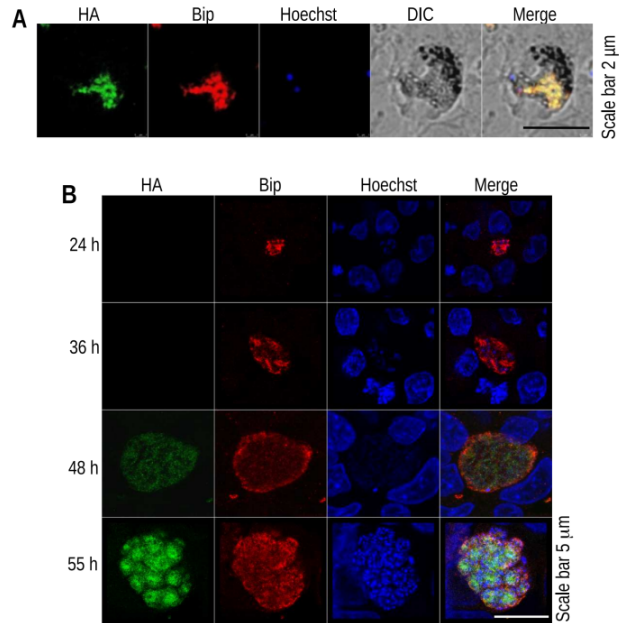
Fig. 1. Localization of *P. berghei* Scd in the parasite endoplasmic reticulum. (A) IFA with asexual blood stage parasites confirmed Scd expression, which colocalized with the endoplasmic reticulum (ER) marker Bip. (B) The expression of Scd was monitored during liver stage development at different time points, and we found late expression of Scd at 48 and 55 hpi, which colocalized with the ER marker BiP. The nuclei were stained with Hoechst.

Fig. 2. *Scd* KO parasites display defects in late liver stage development. (A) To determine the liver parasite burden, sporozoites were injected intravenously into C57BL/6 mice, livers were homogenized at 36, 55 and 72 hpi, RNA was isolated, and transcripts were quantified using real-time PCR. The 18S rRNA copy number was determined and normalized to mouse GAPDH transcripts. The *P. berghei* 18S rRNA copy number was comparable in WT GFP and *Scd* KO parasites at 36 hpi but significantly lower in *Scd*KO parasites than in WT GFP parasites at 55 hpi, and at 72 hpi, it was opposite and found to be significantly higher in KO parasites, indicating that only WT GFP parasites were able to egress from the liver. Similar results were obtained in three independent experiments. Data represent the mean \pm SD, n = 5 mice per group. (B) A lower level of MSP1 transcripts at 55 hpi in KO-infected liver suggests a failure in the maturation of parasites. Data are presented as the mean \pm SEM from two independent experiments (significant difference (p=0.0132), Student's t test).

Fig. 3. *Scd* KO liver stages grow normally. (A) Sporozoite-infected HepG2 cells were fixed at 12, 24, 36, 48, and 62 hpi and immunostained with anti-UIS4 antibody. Nuclei were stained with Hoechst. Visually, liver stage growth appeared to be comparable in *Scd* KO and WT GFP parasites. (B, D and F) The EEF numbers were found to be normal at 36, 48, and 62 hpi (p=0.3950 at 36 hpi, p= 0.9419 at 48 hpi, and p=0.6070 at 62 hpi). (C, E and G) Determination of EEF size at 36, 48, and 62 hpi. The size of EEFs was comparable between WT GFP and *Scd* KO parasites (p=0.5096 at 36 hpi, p=0.6269 at 48 hpi, and p=0.1642 at 62 hpi). The data were pooled from three independent experiments. Data represent the mean \pm SD. P values were determined by an unpaired, two-tailed Student's t test.

Fig. 4. *Scd* KO parasites arrest late during liver stage development and do not form hepatic merozoites. (A) Infected HepG2 cells were harvested at 62 hpi, fixed, and immunostained with anti-merozoite surface protein 1 (MSP1) antibody, and DNA was stained with Hoechst. We found normal segregation of nuclei and formation of merozoites in WT GFP, but it was impaired in *Scd* KO parasites. (B) Counting of nuclei in the EEF revealed impaired nuclear division in KO parasites (p<0.001, Student's t test). The data were pooled from three independent experiments. Data represent the mean \pm SD. (C) The merozoite numbers were counted using a hemocytometer. *Scd* KO parasites formed EEFs that were comparable to WT GFP parasites but failed to form merozoites, a significant difference (p<0.0001, Student's t test).

Fig. 5. Lack of *Scd* leads to defects in organelle morphology and biogenesis. (A) Infected HepG2 cells were fixed at 62 hpi and immunostained with apicoplast marker anti-ACP antibody. WT GFP showed normal branching of the apicoplast, which was impaired in *Scd* KO parasites. (B) Immunostaining of EEFs with an ER marker anti-Bip antibody revealed impaired branching in *Scd* KO parasites.



Hosted file

Fig.2.eps available at <https://authorea.com/users/653075/articles/660231-stearoyl-coa-desaturase-regulates-membrane-biogenesis-and-hepatic-merozoite-formation-in-plasmodium-berghei>

Hosted file

Fig.3.eps available at <https://authorea.com/users/653075/articles/660231-stearoyl-coa-desaturase-regulates-membrane-biogenesis-and-hepatic-merozoite-formation-in-plasmodium-berghei>

